Weathering-limited hillslope evolution in carbonate landscapes

Vincent Godard, Vincent Ollivier, Olivier Bellier, Cécile Miramont, Esmaeil Shabanian, Jules Fleury, Lucilla Benedetti, Valery Guillou

AUTHOR QUERY FORM

ELSEVIER	**Journal:** EPSL	**Please e-mail your responses and any corrections to:**
	Article Number: 13813	**E-mail:** corrections.essd@elsevier.vtex.lt

Dear Author,

Please check your proof carefully and mark all corrections at the appropriate place in the proof (e.g., by using on-screen annotation in the PDF file) or compile them in a separate list. Note: if you opt to annotate the file with software other than Adobe Reader then please also highlight the appropriate place in the PDF file. To ensure fast publication of your paper please return your corrections within 48 hours.

For correction or revision of any artwork, please consult *http://www.elsevier.com/artworkinstructions*

Any queries or remarks that have arisen during the processing of your manuscript are listed below and highlighted by flags in the proof. Click on the 'Q' link to go to the location in the proof.

Location in article	**Query / Remark: click on the Q link to go** **Please insert your reply or correction at the corresponding line in the proof**
Q1	Your article is registered as a regular item and is being processed for inclusion in a regular issue of the journal. If this is NOT correct and your article belongs to a Special Issue/Collection please contact <k.stair@elsevier.com> immediately prior to returning your corrections. (p. 1/ line 1)
Q2	The author names have been tagged as given names and surnames (surnames are highlighted in teal color). Please confirm if they have been identified correctly and are presented in the desired order. (p. 1/ line 14)
Q3	Figs. 1, 4, 5, 8 will appear in black and white in print and in color on the web. Based on this, the respective figure captions have been updated. Please check, and correct if necessary. (p. 3/ line 47)
Q4, Q5, Q6, Q7, Q8, Q9, Q10, Q11	Please provide grant numbers for the sponsors: CEA; ITER; INSU/CNRS; ANR; IRD; CEA (if available) and include these numbers into the main text where appropriate. (p. 10/ line 46,47,48,49,50,51,52,53)
Q12	Please check if sponsor names have been identified correctly and correct if necessary. (p. 12/ line 4)

Please check this box if you have no corrections to make to the PDF file ☐

Thank you for your assistance.

Contents lists available at ScienceDirect

Earth and Planetary Science Letters

www.elsevier.com/locate/epsl

Weathering-limited hillslope evolution in carbonate landscapes

Vincent Godard[a,*], Vincent Ollivier[b], Olivier Bellier[a], Cécile Miramont[c], Esmaeil Shabanian[a,1], Jules Fleury[a], Lucilla Benedetti[a], Valéry Guillou[a], ASTER Team[a,2]

[a] Aix-Marseille Université, CNRS, IRD, CDF, CEREGE UM34, 13545 Aix-en-Provence, France
[b] Aix Marseille Université, CNRS, MCC, LAMPEA UMR 7269, 13094 Aix-en-Provence, France
[c] Aix-Marseille Université, CNRS, IRD, Avignon Université, IMBE UMR 7263, 13545 Aix-en-Provence, France

A R T I C L E   I N F O

Article history:
Received 18 November 2015
Received in revised form 25 February 2016
Accepted 20 April 2016
Available online xxxx
Editor: A. Yin

Keywords:
landscape evolution
carbonates
denudation
cosmogenic nuclides
hillslope processes

A B S T R A C T

Understanding topographic evolution requires integrating elementary processes acting at the hillslope scale into the long-wavelength framework of landscape dynamics. Recent progress has been made in the quantification of denudation of eroding landscapes and its links with topography. Despite these advances, data is still sparse in carbonate terrain, which covers a significant part of the Earth's surface. In this study, we measured both long-term denudation rates using in situ-produced ^{36}Cl concentrations in bedrock and regolith clasts and surface convexity at 12 sites along ridges of the Luberon carbonate range in Provence, Southeastern France. Starting from ~30 mm/ka for the lowering of the summit plateau surface, denudation linearly increases with increasing hilltop convexity up to ~70 mm/ka, as predicted by diffusive mass transport theory. Beyond this point denudation rates appear to be insensitive to the increase in hilltop convexity. We interpret this constant denudation as indicating a transition from a regime where hillslope evolution is primarily controlled by diffusive downslope regolith transport, toward a situation in which denudation is limited by the rate at which physical and chemical weathering processes can produce clasts and lower the hilltop. Such an abrupt transition into a weathering-limited dynamics may prevent hillslope denudation from balancing the rate of base level fall imposed by the river network and could potentially explain the development of high local relief in many Mediterranean carbonate landscapes.

1. Introduction

Our understanding of landscape dynamics relies on the ability to predict rates of denudation from the measurement of topographic properties. The possibility of establishing a causal link between the two has been greatly enhanced over the last two decades, mainly due to several critical methodological breakthroughs. First, the availability of high resolution representations of the topographic surface, through LiDAR or photogrammetric techniques, has allowed the systematic measurement of elevation over length-scales that are relevant for the elementary geomorphic processes at work, in particular across hillslopes (e.g. Roering et al., 1999; Perron et al., 2008). Second, we can now measure in situ-produced cosmogenic nuclides concentrations in various near-surface materials, allowing accurate quantification of the rates of geomorphic processes. The combination of these spatial and temporal constraints has allowed the investigation and validation of several Geomorphic Transport Laws (Dietrich et al., 2003) pertaining to first-order open questions in landscape evolution (e.g. Small et al., 1999; Roering et al., 2007; Hurst et al., 2012; Johnstone and Hilley, 2015; Foster et al., 2015). For example, based on a simple conceptual model for the evolution of soil-mantled hillslopes (Gilbert, 1909; Culling, 1960), field observations of diagnostic relationships between landscape morphology (slope angles, curvature) and rates of evolution (downslope regolith transport, denudation) are direct hints of the occurrence of specific processes (e.g. McKean et al., 1993; Heimsath et al., 1997; Anderson, 2002; Hurst et al., 2012).

Many of the aforementioned studies have focused on the evolution of landscapes developed on quartz-rich lithologies, where the measurement of in situ-produced ^{10}Be concentrations in bedrock or regolith materials provided direct constraints on processes timescales. Recent advances on the calibration of ^{36}Cl production rate from Ca spallation have opened the way for the implementation of similar approaches in carbonate landscapes (Stone et al., 1994; Schimmelpfennig et al., 2009). For example,

* Corresponding author.
E-mail address: godard@cerege.fr (V. Godard).
[1] Now at: Institute for Advanced Studies in Basic Sciences, Gava Zang – Zanjan, Iran.
[2] Maurice Arnold, Georges Aumaître, Didier L. Bourlès, Karim Keddadouche.

http://dx.doi.org/10.1016/j.epsl.2016.04.017

Ryb et al. (2013, 2014b, 2014a) have provided important insights into the spatial distribution of denudation for carbonate dominated landscapes across a strong climatic gradient in Israel. The significant control of the precipitation gradient on the denudation pattern support the idea that dissolution is the major regulator of the evolution of such landscapes and that physical processes play only a secondary role, unless water availability becomes limiting for chemical weathering. However, in many carbonate landscapes hillslopes display convex hilltops that are commonly associated with diffusion-like regolith transport (Gilbert, 1909; Culling, 1960). These observations suggest that physical weathering and regolith transport may play a significant role in the evolution of carbonate hillslopes in addition to total dissolution. Due to their frequent occurrence, especially in peri-Mediterranean regions, it is of major interest to understand the dynamics of carbonates dominated landscapes, in particular to assess to what extent the evolution processes and Geomorphic Transport Laws that have been proposed and validated for soil mantled hillslopes are transferable to these settings.

The purpose of this study is to provide such quantitative insights into the dynamics of these landscapes and hillslopes through the combination of detailed morphological measurements with estimates of denudation based on in situ-produced cosmogenic nuclides inventories. We focused on the carbonate ranges of Provence in South-Eastern France which provide an ideal setting for such investigations. In particular we test if the fundamental relationship between surface curvature and denudation, which is often considered diagnostic of diffusive transport over regolith-mantled hillslopes, holds in this type of environments. We observe a two-stage evolution, with first a linear increase of denudation rates with hilltop curvature, as predicted by linear diffusion transport theory, and then a plateau where denudation is almost constant despite increasing curvature. We interpret this transition as the consequence of a limit in the ability of weathering processes to produce regolith fast enough to match hillslope transport capacity. We postulate that such evolution could lead to the decoupling of hillslopes evolution from the channels incising at their bottom and promote relief growth in carbonate landscapes.

In this paper, we first present the geological and geomorphological settings of the carbonate ranges of Western Provence, and in particular the Luberon massif where our investigation is focused. After presenting the methodology used to determine denudation rates from cosmogenic nuclides (^{36}Cl) measurements and hilltop curvature from the production of high resolution Digital Elevation Models, we introduce a simple 1D hillslope evolution model that allows combining the data obtained by both previous methods. At last, after reporting the main data and results we discuss the significance of the observed transition for the mechanisms of landscape evolution in carbonate domains.

2. Setting

The sedimentary sequence of Western Provence is dominated by a thick Mesozoic platform carbonate series that was deformed during Cenozoic orogenesis. This led to the development of narrow ranges with significant relief, which provide an ideal setting to investigate the evolution of carbonate landscapes (Fig. 1A). We targeted an area of the Western Luberon mountain (Petit Luberon, Fig. 1B), a 600 m tall, E-trending and 20 km-long range. It consists mostly of lower Cretaceous carbonates, with Urgonian facies reef limestones outcropping along the crest and northern flank of the range. The Luberon mountain was first uplifted during the Late Cretaceous and Early Eocene Pyrenean tectonic regime. Another major tectonic episode occurred between 10 and 6 Ma prior to the Messinian Salinity Crisis, and led to rejuvenation of the relief and incision (Molliex et al., 2011; Clauzon et al., 2011). Denudation rates on weathering surfaces across south-eastern France ranges from 20 to 60 mm/ka (Siame et al., 2004; Sadier et al., 2012; Molliex et al., 2013). The lower bound corresponds to tectonically stable areas, whereas higher values are associated with actively uplifting surfaces.

We selected a specific area of the northern flank of the range, where several regularly spaced north-south ridges are connected with a summit surface (Fig. 1C). Their well-developed convex profiles suggest that slope-dependent transport is likely contributing to hillslope evolution (Fig. 2A–B). The low curvature summit surface is being progressively dismantled by regressive erosion along the main valleys draining the southern and northern flanks. This transient evolution is also reflected in the morphology of the ridges, which show significant increases in convexity with distance from the summit (Fig. 1C). Hillslopes become steeper away from the main crest and ultimately develop steep cliff faces associated with narrow gorges in the lower part of the range (Figs. 1 and 8).

The climate consists of a combination of Mediterranean and continental characteristics. Available records in Bonnieux (Altitude 250 m asl, Fig. 1B) over the 1981–2010 period indicate mean annual precipitation is 750 mm/yr, mean minimum annual temperature is 8 °C (1 °C between December and February) and frost is present for 50 days per year. Our sites are located much higher on the crest of the range, between 600 and 700 m asl, and are directly exposed to the dominant wind (North–South blowing *Mistral*), suggesting that the conditions they experience are likely to be significantly colder. The ridges host sparse Mediterranean vegetation characterized by small shrubs and shallow grass. The surface is covered by thin but dense regolith (<10 cm in most places) consisting of limestone clasts in the 1–10 cm size range and discontinuous shallow sandy to silty soil pockets (10 to 20 cm deep in most places) (Fig. 2). The dimension of these clasts make them transportable by biotic and frost wedging processes. Bedrock outcrops are widespread along these ridges and display a dense network of incipient dissolution features that contribute to clast production. This joint occurrence of meter-scale bedrock patches and thin discontinuous regolith is observed both on hilltops and hillslope flanks, with no clear downslope thinning or thickening trend for the regolith layer.

Bedrock and regolith observed along the crests have undergone both chemical weathering and physical disaggregation. Dissolution features are widespread on both bedrock outcrops and regolith clasts (Fig. 2E–F). Carbonate dissolution contributes to the progressive rounding of rock fragments and to the development and widening of a network of discontinuities in the rock mass (lapiaz) which in many cases produces transportable clasts. There is also widespread evidence of active fracture development (Fig. 2C), which appears to be related to thermal stresses and frost cracking but is also probably assisted by bioturbation and the development of the root network. We note that the production of clasts is also greatly facilitated by pre-existing tightly spaced fracture planes that are prevalent at most bedrock outcrops (Fig. 2D).

3. Methods

3.1. Sampling strategy

We focus on a single area within which relationships between denudation and morphology can be isolated under constant climate and lithology. Our sites are located on top of the ridges, where no regolith flux from above is contributing to the hillslope evolution. We use in situ-produced ^{36}Cl concentrations measured in both bedrock and regolith fragments (1–10 cm size range) to quantify denudation rates at 12 sites. ^{36}Cl accumulates in near surface carbonates mainly due to nuclear reactions induced by cosmic

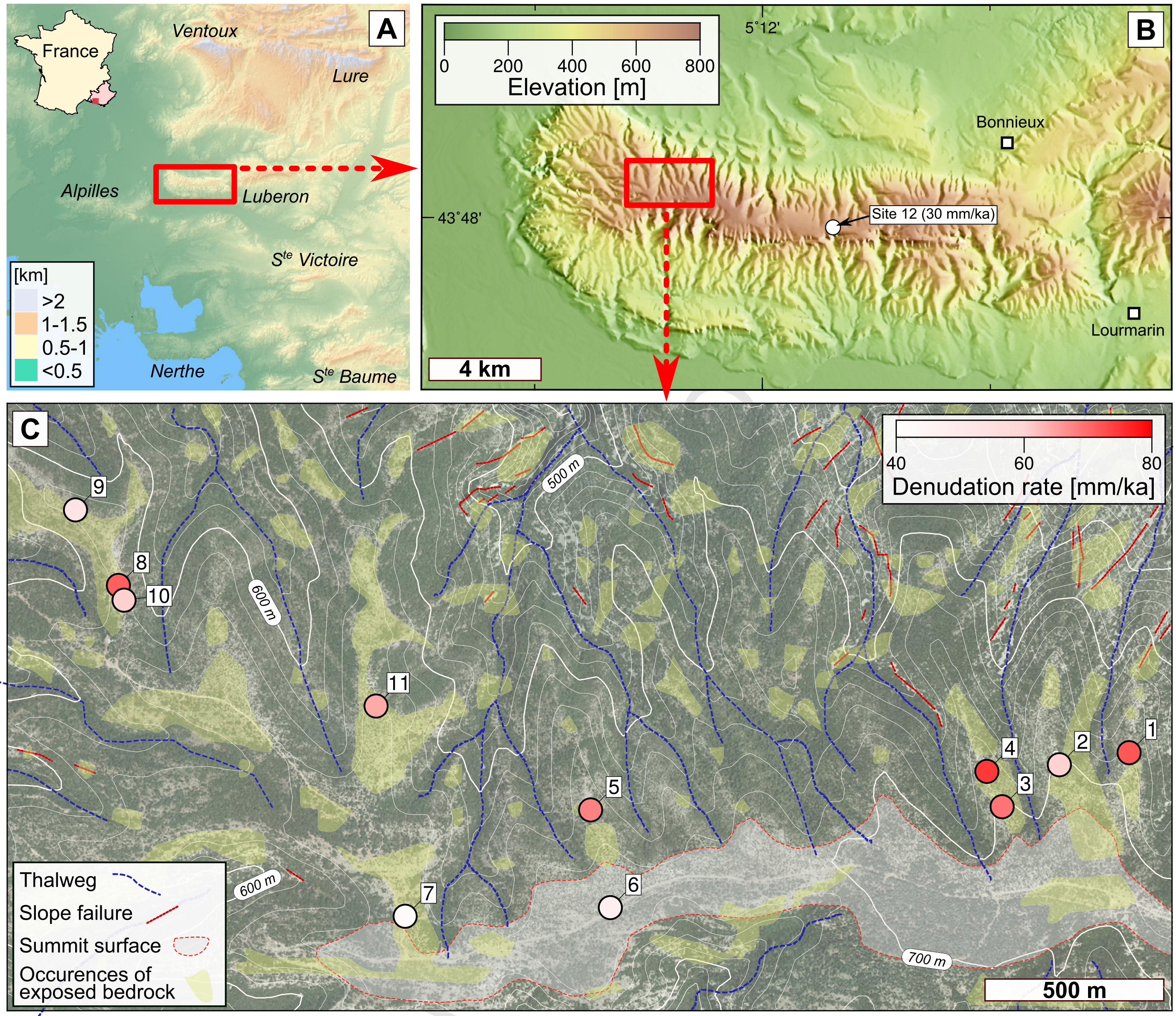

Fig. 1. A – General situation map of the studied region (Provence, south-eastern France), with the location of the main carbonate ranges. B – Situation map of the Petit Luberon mountain (IGN BDALTI DEM). C – Orthophotography of the main sampling area (IGN BDORTHO database), and main geomorphological features based on field surveys and air photos analysis. Samples are color coded according to their denudation rate. Thin white contour lines separation is 20 m. Site 12 was sampled farther east, where the summit surface is the widest. (For interpretation of the references to color in this figure, the reader is referred to the web version of this article.)

ray interaction with Calcium. Hilltop curvature was determined using Digital Surface Models derived from pairs of high resolution aerial photographs at the same sites where we obtained estimates for denudation rates.

3.2. Sample preparation and measurements

Chlorine was extracted from our samples according to the standard protocol used in CEREGE (Schlagenhauf et al., 2010). Bedrock and amalgamated clasts samples were crushed and sieved to extract the 250–1000 μm fraction. For each sample ∼50 g were loaded in Nalgene bottles and were submitted to three 5-hours cycles of leaching with MQ water and mechanical shaking. Further sample cleaning was done with a HNO_3 (2M) leaching, resulting in the dissolution of ∼10% of the sample mass. The samples were then dried, weighted and spiked with ∼0.3 g of a Cl solution, with a concentration of 6.92 ± 0.05 mg/g and $^{35}Cl/^{37}Cl$ and $^{36}Cl/^{37}Cl$ ratios of 917.8 ± 4.4 and $2.72 \pm 0.50 \times 10^{-12}$, respectively. Total dissolution of the carbonates was performed with HNO_3 (2M). The solution was filtered and the residues weighted. We then added ∼3 ml of an $AgNO_3$ solution (100 mg/g) for AgCl precipitation (3 days storage in the dark). The precipitate was dissolved in NH_4OH (1:1) and ∼1 ml of $Ba(NO_3)_2$ solution was added for sulfate precipitation. Filtering allowed to remove the $BaSO_4$ precipitate, and final AgCl precipitation was achieved by adding ∼2 ml NNO_3 (1:1). The precipitate was dried and stored in the dark until its final loading in targets for AMS measurements.

Measurements of the chlorine isotopic ratios were performed at the French AMS National Facility, ASTER, located at CEREGE in Aix-en-Provence (Merchel et al., 2008; Arnold et al., 2013). A KN-STD1600 standard was used with assigned ratios for $^{36}Cl/^{35}Cl$, $^{36}Cl/^{37}Cl$ and $^{35}Cl/^{37}Cl$ of 2.112×10^{-12}, 6.603×10^{-12} and 3.127, respectively (Sharma et al., 1990; Fifield et al., 1990).

Please cite this article in press as: Godard, V., et al. Weathering-limited hillslope evolution in carbonate landscapes. Earth Planet. Sci. Lett. (2016), http://dx.doi.org/10.1016/j.epsl.2016.04.017

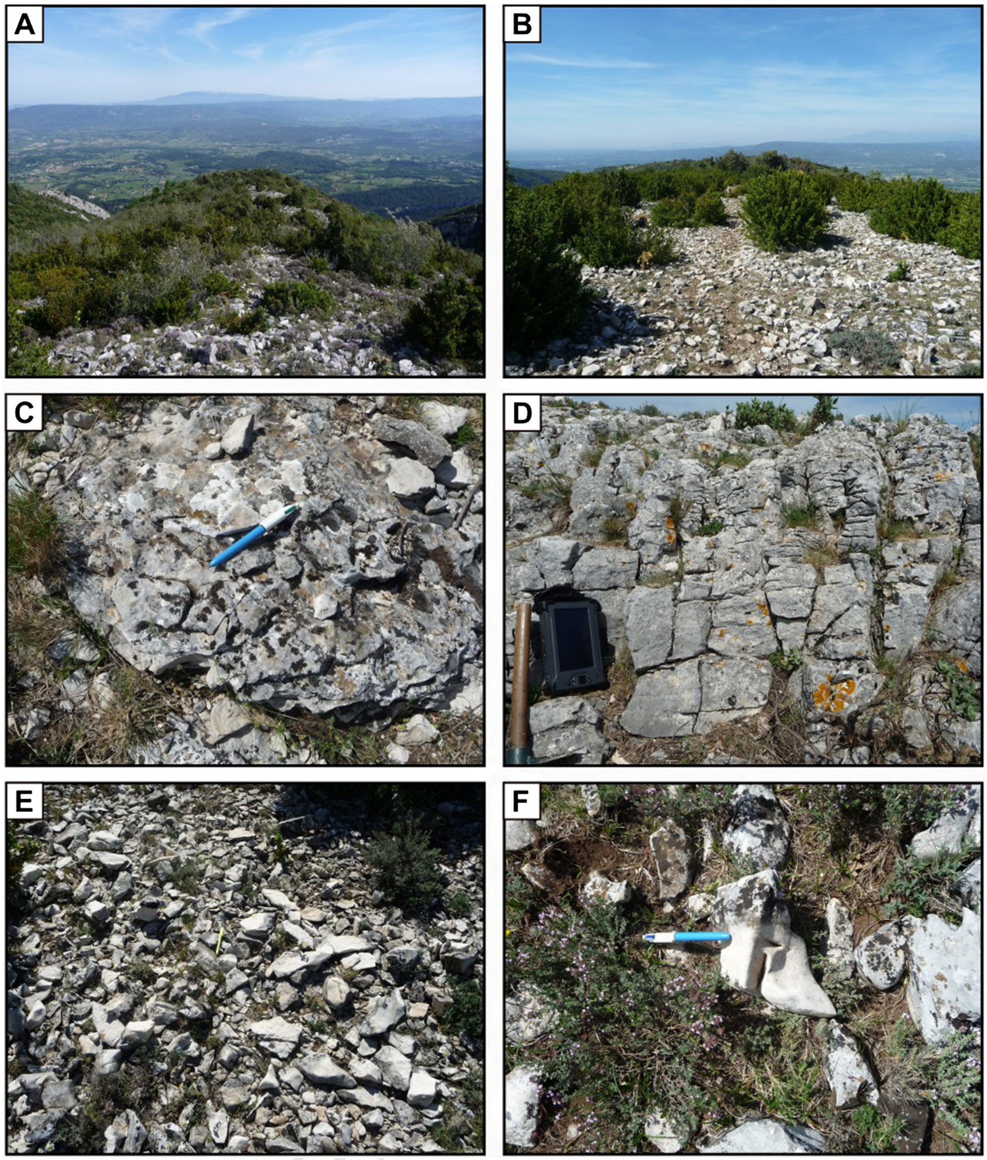

Fig. 2. Field photographs illustrating geomorphological features of the Petit Luberon northern flank. A–B – Views along the ridge axis looking toward the north for sites 1 and 11, respectively. C – In-situ frost or bioturbation assisted fracturing contributing to the separation of individual clasts from the bedrock, observed at site 10. D – Pre-existing fractures and structural bedding contributing to the separation of individual clasts from the bedrock, observed at site 8. E – View of clasts pavements at the surface of site 2. F – Weathered and rounded clasts at the surface of site 8, showing a clear distinction between the lower part of the clast embedded in the regolith (white, rounded and polished surface) and the upper part directly exposed at the surface (grayish surface partly covered with lichens).

3.3. Hilltop curvature measurements

New algorithms in photogrammetry have allowed this technique to emerge as an alternative tool to LiDAR in studies requiring very high resolution topography. Advances in computer vision and image analysis have generated innovative developments in photogrammetry through Structure-from-Motion (SfM) technique, which offers an automated method for the production of high-resolution models with standard cameras (e.g. James and Robson, 2012; Westoby et al., 2012). This is achieved with calibrated cameras knowing the extrinsic orientation parameters. The identification of tie points between image pairs is done automatically and efficiently using the Scale Invariant Feature Transform (SIFT) algorithm, and the results are optimized and converted in an absolute reference frame using ground control points known precisely in a geodetic system. Then the transform from image to object geometry is performed by bundle rays block adjustment. It consists in a cost optimization function for the 3D structure and the viewing parameters. The outputs of the methods are primarily a dense 3D point cloud, and one can produce also a Digital Surface Model and an orthophotography by projecting the point cloud on a defined plane.

We used aerial photographs acquired by the Institut Géographique National (IGN), that were processed with Agisoft Photoscan Professional software suite to generate a high density point cloud. The sparse vegetation of this area allows a bare-Earth terrain model to be created, with only limited clipping of isolated bushes required. The point cloud was registered in RGF93, resulting in a typical density of 2.7 ± 1.1 points/m^2.

Calculations were performed on the point cloud in circular neighborhoods centred around the sampling sites along the ridges. The size of this neighborhood is based on the transition between the short wavelength signal associated with surface roughness and vegetation to the long wavelength signal of ridge and valley topography (Roering et al., 2010; Hurst et al., 2012), and in our case was set to 15 m (Fig. 4). Changing this radius in the 10–30 m

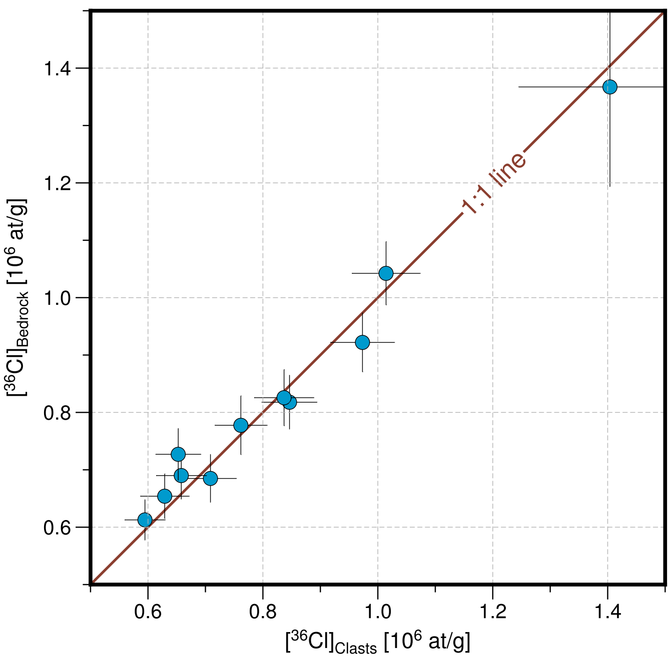

Fig. 3. Comparison of ^{36}Cl concentrations in bedrock and amalgamated clasts samples at a same location.

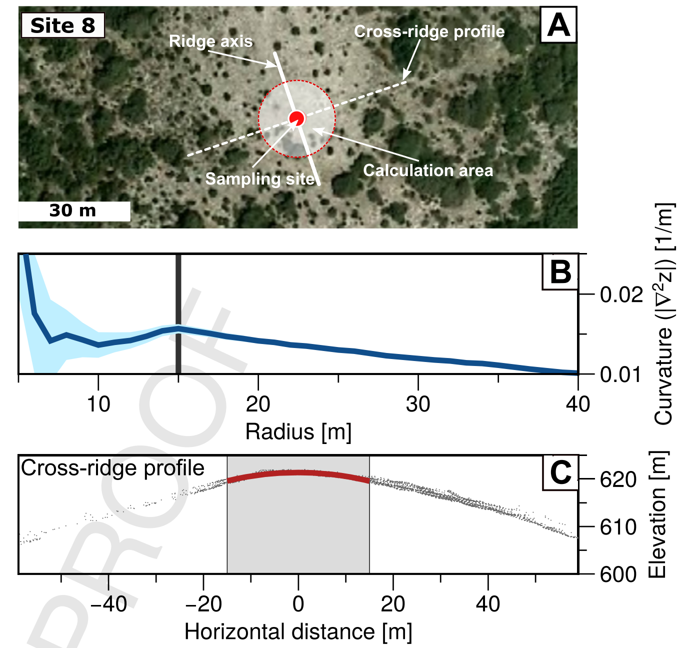

Fig. 4. A – Aerial view of sampling site 8 (Fig. 1C), with sampling location and radius of calculation (15 m) for the curvature. B – Evolution of calculated curvature at site 8 with the radius of the calculation area. Light blue envelope indicates the $\pm 1\sigma$ interval. Dark vertical line indicates the reference radius used in this study. C – Cross ridge topographic profile at site 8 (light gray points). Dark gray background indicates the calculation area for curvature corresponding to a 15 m radius around the sampling site. Solid thick red curve is quadratic fit through the data points. (For interpretation of the references to color in this figure legend, the reader is referred to the web version of this article.)

range or performing the calculation on the gridded Digital Elevation Model rather than on the point cloud slightly modified the values of the computed curvatures, but did not affect the general first-order trend in the dataset. We follow the approach of Hurst et al. (2012, 2013b) by fitting a quadratic surface to the neighborhood around our sampling site,

$$z(x,y) = ax^2 + by^2 + cxy + dx + ey + f \tag{1}$$

And curvature C can be expressed from the coefficients of equation (1) as,

$$C = 2a + 2b \tag{2}$$

3.4. Hillslope evolution model

We develop a simple hillslope evolution model to understand the relations between denudation and curvature in this landscape. Geomorphic Transport Law (GTL)-based models of hillslope evolution have been extensively applied to the investigation of the behavior of soil mantled landscapes in most situation underlain by silicate rich substrata (e.g., Anderson, 2002; Dietrich et al., 2003; Roering et al., 2004; Mudd and Furbish, 2004; Roering, 2008; Yoo et al., 2009; Pelletier and Perron, 2012; Pelletier et al., 2013). We are well aware that carbonate landscapes have, in comparison, received far less attention, and that the formulation of some processes are not yet completely validated in such environments. With these limitations in mind, our purpose is not to perform an extensive parameter space exploration, but rather to test the implications of simple assumptions for processes operating at the scale of the hillslope.

Our model is based on a simple statement of conservation for the regolith cover (thickness h) transported downslope (e.g. Anderson, 2002). The evolution of h through time can be described by,

$$\frac{\mathrm{d}h}{\mathrm{d}t} = \frac{\rho_b}{\rho_r}\dot{W} + \frac{1}{\rho_r}\frac{\mathrm{d}q_s}{\mathrm{d}x} - p_d h \tag{3}$$

The first right hand term is a source associated with production of regolith from the underlying bedrock. We use a simple regolith production function based on an exponential decay (length scale L_0) of production with regolith thickness (h) and a maximum production E_0 for exposed bedrock,

$$\dot{W} = \frac{E_0}{\cos\theta}\exp\left(\frac{-h\cos\theta}{L_0}\right) \tag{4}$$

The local slope is θ, and the $\cos\theta$ maps vertical thickness into slope normal thickness. This formulation is based on extensive work in silicate-rich soil-mantled landscapes (Heimsath et al., 1997, 2000), but we are aware that other formulations have been proposed (e.g. Small et al., 1999; Anderson, 2002; Carretier et al., 2014).

The second right hand term represents the regolith flux q_s that evolves non-linearly with topographic gradient ∇z (Roering et al., 1999, 2007; Roering, 2008), and is linearly dependent on regolith thickness (Pelletier et al., 2013),

$$q_s = -\frac{K_T h \cos\theta \nabla z}{1 - (\frac{\nabla z}{Sc})^2} \tag{5}$$

K_T is a transport coefficient [L/T] and S_c [L/L] a critical slope gradient at which regolith flux goes to infinity.

Finally, we parametrize regolith dissolution during its downslope transport as a first-order kinetic process characterized by a constant rate p_d of mass loss per units of mass and time.

4. Data and results

4.1. Denudation rate measurements with ^{36}Cl

Denudation rates were calculated from ^{36}Cl concentrations, based on spatial scaling factors from Stone (2000) and using the approach and parameters of the procedure proposed by Schimmelpfennig et al. (2009) which relied on the Heisinger et al. (2002) muon schemes. The natural Cl concentration of all samples is lower than 10 ppm and mostly between 4 and 2 ppm, the

Table 1
Analytical results for the samples processed in this study.

Site	Type	Latitude	Longitude	Altitude (m)	[^{36}Cl] (10^6 at/g)	[Ca] (%)	[Cl] (ppm)	Denudation (mm/ka)
1	Clasts	5.1587	43.8059	684	0.64 ± 0.02	31	2	71.9 ± 7.5
2	Clasts	5.1516	43.8059	706	0.85 ± 0.02	40	2	57.7 ± 6.0
	Bedrock				0.82 ± 0.02	40	3	60.2 ± 6.3
3	Clasts	5.1421	43.8143	707	0.71 ± 0.02	41	2	71.0 ± 7.5
	Bedrock				0.69 ± 0.02	34	2	69.1 ± 7.2
4	Clasts	5.1407	43.8163	694	0.59 ± 0.02	26	2	74.6 ± 7.8
	Bedrock				0.61 ± 0.02	30	2	74.6 ± 7.8
5	Clasts	5.1508	43.8111	672	0.66 ± 0.02	21	6	66.2 ± 7.0
	Bedrock				0.69 ± 0.02	31	7	67.7 ± 7.1
6	Clasts	5.1422	43.8140	687	0.97 ± 0.03	30	4	44.2 ± 4.6
	Bedrock				0.92 ± 0.03	31	4	47.6 ± 4.9
7	Clasts	5.1768	43.8095	680	1.01 ± 0.03	29	3	41.0 ± 4.3
	Bedrock				1.04 ± 0.03	35	4	42.6 ± 4.4
8	Clasts	5.1744	43.8092	622	0.63 ± 0.02	31	6	72.1 ± 7.6
	Bedrock				0.65 ± 0.02	33	7	71.1 ± 7.4
9	Clasts	5.1724	43.8082	624	0.84 ± 0.03	32	3	51.7 ± 5.4
	Bedrock				0.83 ± 0.02	33	3	52.9 ± 5.5
10	Clasts	5.1719	43.8091	625	0.76 ± 0.02	36	8	61.5 ± 6.4
	Bedrock				0.78 ± 0.03	34	10	60.4 ± 6.4
11	Clasts	5.1582	43.8084	663	0.65 ± 0.02	35	5	73.3 ± 7.7
	Bedrock				0.73 ± 0.02	32	7	64.1 ± 6.7
12	Clasts	5.231	43.797	660	1.40 ± 0.08	39	2	29.8 ± 3.4
	Bedrock				1.37 ± 0.09	38	2	30.9 ± 3.7

main production pathway for ^{36}Cl is thus through Ca spallation. All analytical results are provided in Table 1.

Two process blanks were treated and measured along with our samples. They contained 0.123×10^6 and 0.068×10^6 atoms of ^{36}Cl which is two orders of magnitude lower than the $31.2 \pm 5.6 \times 10^6$ average value in our samples. They contained 0.052×10^{18} and 0.095×10^{18} atoms of natural chlorine which is at least one order of magnitude lower than the $3.11 \pm 1.59 \times 10^{18}$ average value in our samples.

Measured concentrations range from 0.6 to 1.4×10^6 at/g, which corresponds to denudation rates in the 30–70 mm/ka range and integrated time periods of 20 to 9 ka, respectively. The ^{36}Cl concentrations and their corresponding denudation rates are similar within 1σ uncertainty for the bedrock and clasts samples, except at site 11 where the discrepancy is of about 10% (Fig. 3). We note variations in the Ca content of our samples of 30–40%, with one sample as low as 21%, which denote a significant dolomitic component at some sites (Table 1). However, such variability in the rock composition does not seem to affect the observed denudation rates.

4.2. Evolution of hilltop curvature with denudation rates

Curvatures values measured at our sites range from $\sim$0 m^{-1} at sites 6 and 12 to $\sim$0.05 m^{-1} at site 4. Denudation rates progressively increase with hilltop curvature (Fig. 5). Starting from 30–40 mm/ka, a nearly linear trend is observed between curvature and denudation rate, consistent with transport-limited diffusive hillslope evolution. Such downslope displacement of the regolith is likely accomplished by bioturbation associated with root development (Hoffman and Anderson, 2014) and freeze-thaw cycles.

For hillslope curvature larger than $\sim$0.02 m^{-1} denudation rates do not increase substantially above $\sim$70 mm/ka, despite a two-fold increase in curvature. This plateau results from a behavioral change of the hillslope in which the rate of regolith production from the bedrock reaches its maximum value and cannot further increase, while curvature continues to evolve because of the ongoing hillslope relief development associated with progressive dissection and incision at the gully bottoms (e.g. Hurst et al., 2013a).

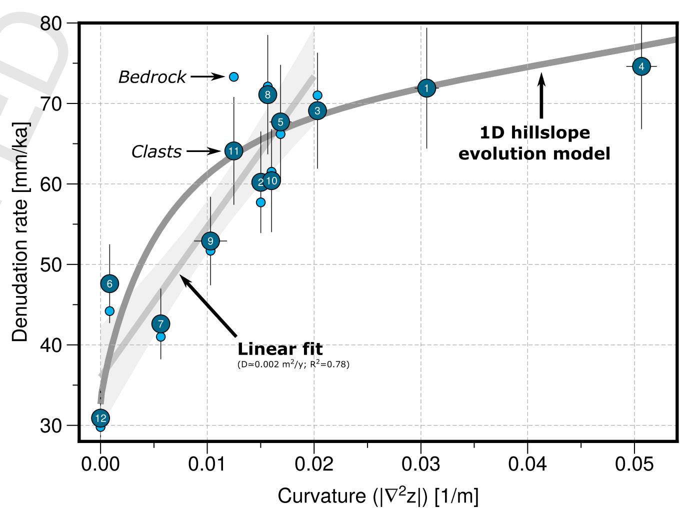

Fig. 5. Denudation rates against hilltop curvature measured at our sampling sites. Large dark blue circles represent denudation rates measured from amalgamated clasts samples, whereas small light blue circles represent bedrock samples. The dark gray background curve is a prediction from a 1D diffusive hillslope evolution model (Fig. 6). The light gray line and envelope (95% confidence) are a linear fit through the data for curvature <0.02 m^{-1}. (For interpretation of the references to color in this figure legend, the reader is referred to the web version of this article.)

4.3. Modelling results

We define our reference model with a set of parameters that allows to reproduce the main characteristics of our dataset. We model the evolution of a 50 m long hillslope and impose, as a boundary condition, the lowering of the base level at a constant rate (100 mm/ka) at the bottom of the hillslope, which corresponds to a progressive and continuous incision of the channels.

We use a transport coefficient of 0.05 m/yr, which is not dimensionally equivalent to a diffusivity coefficient due to the linear dependence on regolith thickness of the transport law presented at equation (5) (Roering, 2008; Pelletier et al., 2013). The critical hillslope gradient S_c is 0.8 and the bedrock-to-regolith density ratio of 1.5. The regolith production function (equation (4)) is parametrized using a standard decrease length scale L_0 of 0.5 m and a maximum

Please cite this article in press as: Godard, V., et al. Weathering-limited hillslope evolution in carbonate landscapes. Earth Planet. Sci. Lett. (2016), http://dx.doi.org/10.1016/j.epsl.2016.04.017

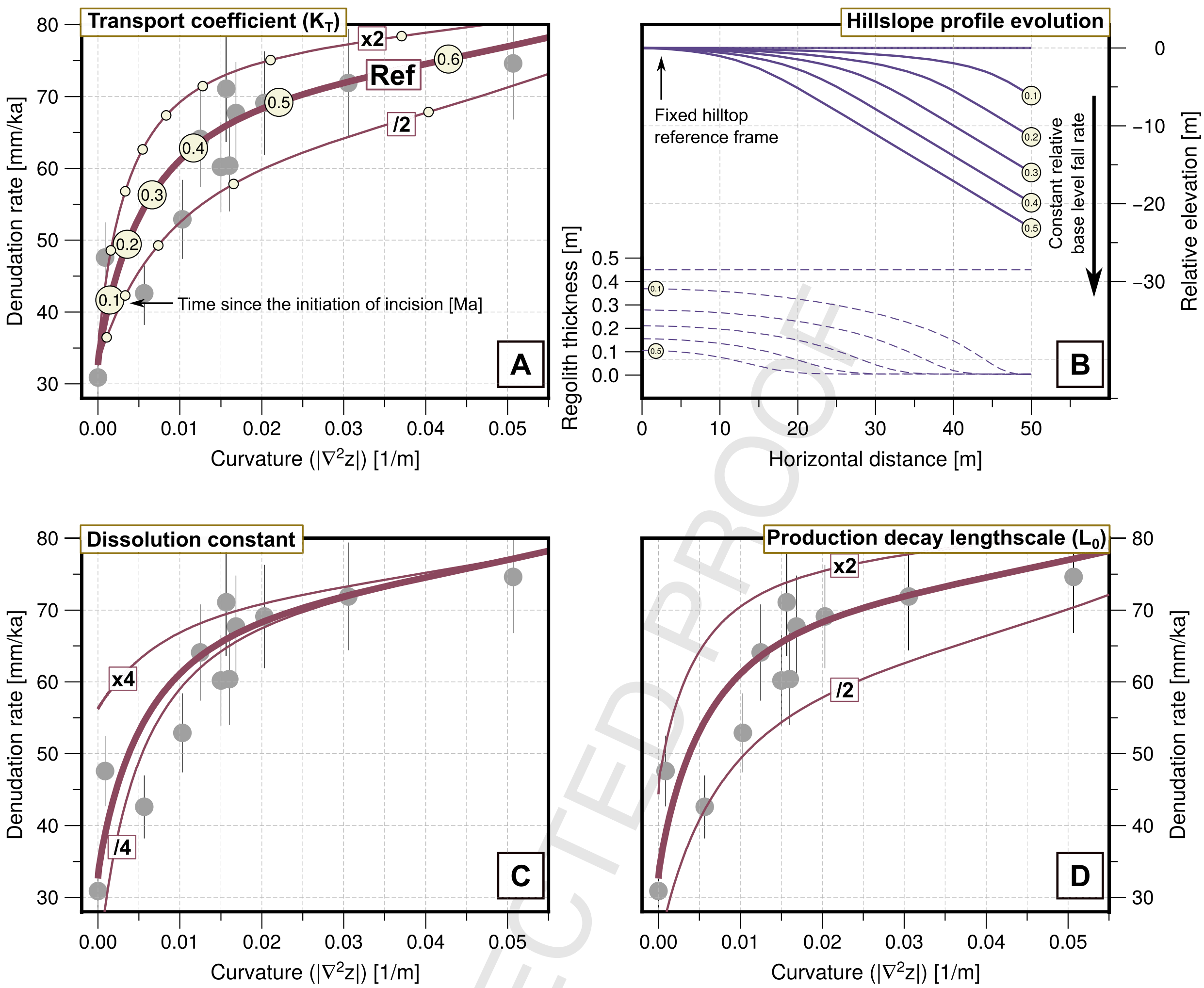

Fig. 6. Modelling results. In all insets A, C and D the thick line is the reference model. Grey circles in the background are the data points for the several sites presented in this study (Fig. 5). A – Test of the influence of 2-fold variations for the transport coefficient K_T (reference value 0.05 m/yr). Dots along the curves are indicating 100 kyr time intervals since the initiation of channel incision at the base of the hillslope. B – Hillslope topography evolution (top) and regolith thickness (bottom) at the time intervals indicated on inset A (constant lowering rate of 100 mm/kyr). All topographic profiles have their hilltops aligned as a reference (hilltop surface are actually progressively lowered with respect to their initial position by dissolution). C – Test of the influence of 4-fold variations of the regolith dissolution rate (reference value 0.01%/yr). D – Test of the influence of 2-fold variations of the e-folding decay length-scale of the regolith production function L_0 (reference value 0.5 m).

rate of surface lowering E_0 of 80 mm/ka. For an horizontal stable surface equation (3) is simply,

$$\frac{\rho_b}{\rho_r} E_0 \exp\left(\frac{-h}{L_0}\right) = p_d h \tag{6}$$

This equation has no analytical solution, but can be numerically solved. Using a regolith dissolution rate of 0.01% per year produces a surface lowering of ∼30 mm/ka, close to observed values in the Luberon summit surface and elsewhere in peri-Mediterranean regions (Furlani et al., 2009; Ryb et al., 2014b, 2014a).

The model displays a rapid increase of denudation at low curvature and then a slower evolution when reaching denudation rates of 60–80 mm/ka (Fig. 6A), which is close to the maximum regolith production E_0 and represents a transition toward a situation where the evolution of the system is limited by the capacity of the hillslope to produce regolith. The associated topographic evolution (Fig. 6B) shows a progressive increase of relief with the development of hilltop curvature, while the base of the hillslope is continuously lowered.

The use of lower or higher transport coefficients results in less or more rapid increase of denudation with curvature during the early stage of the hillslope evolution, respectively (Fig. 6A). The differences in rates of change in denudation become narrower at latter stages when threshold processes are dominating the regolith transport. Variations in regolith dissolution rates are mostly influencing the rate of denudation of the initial flat surface, from almost no lowering for very low dissolution rate to rates up to 60 mm/ka at dissolution equivalent to 4 times the reference value (Fig. 6C). Finally, variations in the characteristic length controlling the dependence of the regolith production on depth (equation (4), Fig. 6D) are shifting the response curve toward slower or faster evolution for lower or higher values, respectively.

Again, we strongly argue against any over-interpretation of these modelling results, as we acknowledge that some model components such as the regolith production rule are still largely unconstrained in carbonate landscapes. Our approach is mainly heuristic and a thought experiment aimed at providing a general framework for the analysis of the behavior of such hillslope. A systematic investigation of the values of specific parameters, beyond the simple sensitivity tests presented in Fig. 6, is clearly not the objective of this model.

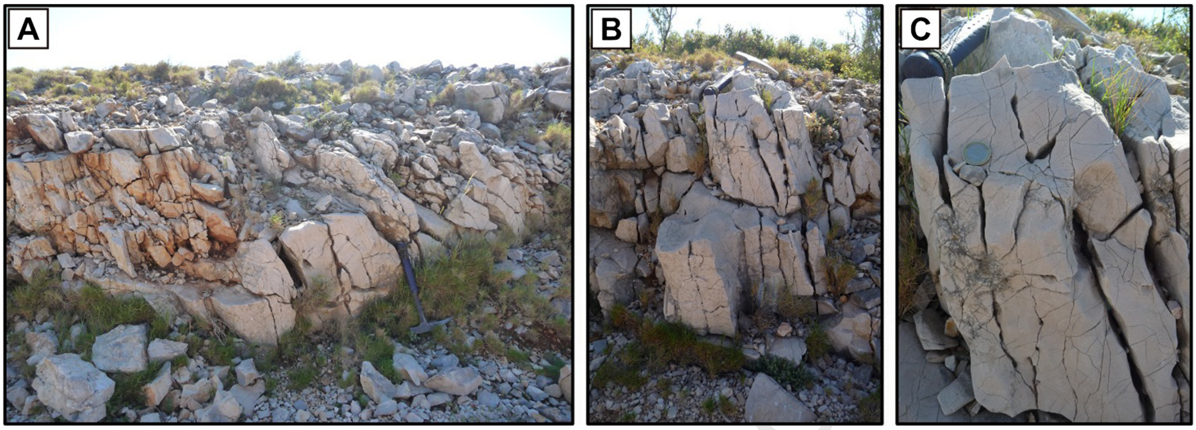

Fig. 7. Field photographs of a bedrock section in the Nerthe massif (west of Marseille, N43.3437–E5.2397). See Fig. 1A for location. A – General view of the section showing the difference in bedrock fracturing with depth. B–C – Closer view illustrating the smoothing action of carbonate dissolution on fracture edges.

5. Discussion

5.1. Interpretation of denudation rates and controlling factors

Our rates are within the range of denudation rate values reported in global compilations (Ryb et al., 2014a). Over flat to low-convexity surfaces, the lower bound of 30 mm/ka is slightly higher than other estimates on carbonate plateaus under Mediterranean climate (e.g. Furlani et al., 2009; Sadier et al., 2012). The fact that ^{36}Cl concentrations (and hence denudation rates) are comparable for bedrock and amalgamated clasts sampled at identical locations has important implications for the evolution of the regolith cover of these ridges over the time period integrated by the method. We argue that this suggests the clasts are not remnants of a thicker soil or regolith that would have been recently eroded away due to a change in climate or land use, which would have produced lower concentrations in the buried and recently exhumed bedrock than the clasts. We therefore make the assumption that the present observed conditions can be extrapolated over at least the last 9 ka, which is the lowest reported integrated time period at our sites.

We could also consider an alternative possibility, where the clasts were previously located close to the interface between the bedrock and a thicker soil layer, that was eroded at some point during the Holocene (e.g. Fuchs, 2007). Several lines of evidence are inconsistent with this hypothesis. First, our sites are located along hillcrests, with some of them presenting a high curvature (Fig. 2A) where the presence of thick soil is unlikely (e.g. Heimsath et al., 1997). Second, such rapid transfer of soil from the hillslopes to the adjacent channels is likely to exceed the local transport capacity but we did not observe significant accumulation in the valley bottoms and hollows of the northern flank of the Petit Luberon. Finally, even if the clasts had been located at the bottom of a previous thicker soil cover, they would still be stratigraphically above the bedrock surface and vertically spread over a few tens of centimeters. The well constrained exponential decrease of spallogenic production of ^{36}Cl with depth would unambiguously lead to significantly lower ^{36}Cl concentrations in the bedrock and a corresponding systematic deviation below the 1:1 line in Fig. 3, which is not what we observe.

The limiting factors on carbonate dissolution have already been thoroughly investigated by Ryb et al. (2014b, 2014a, 2015) across the Mediterranean and arid landscapes of Israel. Mean annual precipitation is 700 mm/yr over the Luberon Mountains, where water availability is likely to be limiting chemical weathering processes (Ryb et al., 2014a). This suggests that physical weathering develops in part because carbonate dissolution alone does not effectively limit relief development. We observe that both physical and chemical processes operate at our sites, in particular that dissolution develops small-scale karstic networks into the rock mass that then allow release of individual clasts (Figs. 2 and 7). We hypothesize that the maximum observed denudation corresponds to a limit in the capacity of the hillslope to dissolve the carbonate substrata and to produce regolith from bedrock. The coupling of physical and chemical processes does not allow us to unambiguously associate this limit to one type of weathering or another. This maximum value of ~70 mm/ka is relative to the specific climatic and lithological conditions at our sites, and for example, higher precipitation would probably increase this limit. In terms of hillslope-scale evolution, this behavioral change corresponds to a transition from a transport-limited to a weathering-limited regime. While we have not carried a quantitative investigation of this parameter, it appears that bedrock exposures are significantly more widespread at the high curvature sites 1 and 4, when compared with other surveyed locations.

5.2. Regolith production and transport processes

The hillslope evolution model generally reproduces the first-order evolution of curvature and denudation observed at the field sites, and in particular the two-stages evolution, with a near-stabilization of denudation at high curvature (Fig. 6). In the model, the presence of this limit is a direct consequence of the existence of maximum regolith production E_0 in equation (4). We postulate that the evolution observed in our cosmogenic and topographic observations is the manifestation of underlying processes presenting a similar behavior with respect to the evolution of the hillslope and regolith layer. While the actual nature of these processes is debated, it can be proposed that they are characterized by a limit corresponding to the maximum rate at which they can operate to lower the bedrock and produce regolith elements.

Field observations in another carbonate massif in Western Provence (Nerthe range, Fig. 1A) provide some clues on the evolution of the shallow bedrock level (Fig. 7). We observe a transition in the degree of fracturing of the bedrock over the first meter below the surface. The uppermost part of the section displays a high fracture density which corresponds to the production of individual clasts in the 1–10 cm size range, that will be the main constituents of the regolith. Deeper in the section (20–30 cm below the surface) the spacing between fractures increases, and the bedrock appears to have been through a lesser degree of mechanical weathering. Closer views confirm that chemical and mechanical processes are jointly operating to produce the clasts, as the fracture edges are significantly smoothed by dissolution (Fig. 7B–C). These observations suggest that the processes that drive the fracturing of the

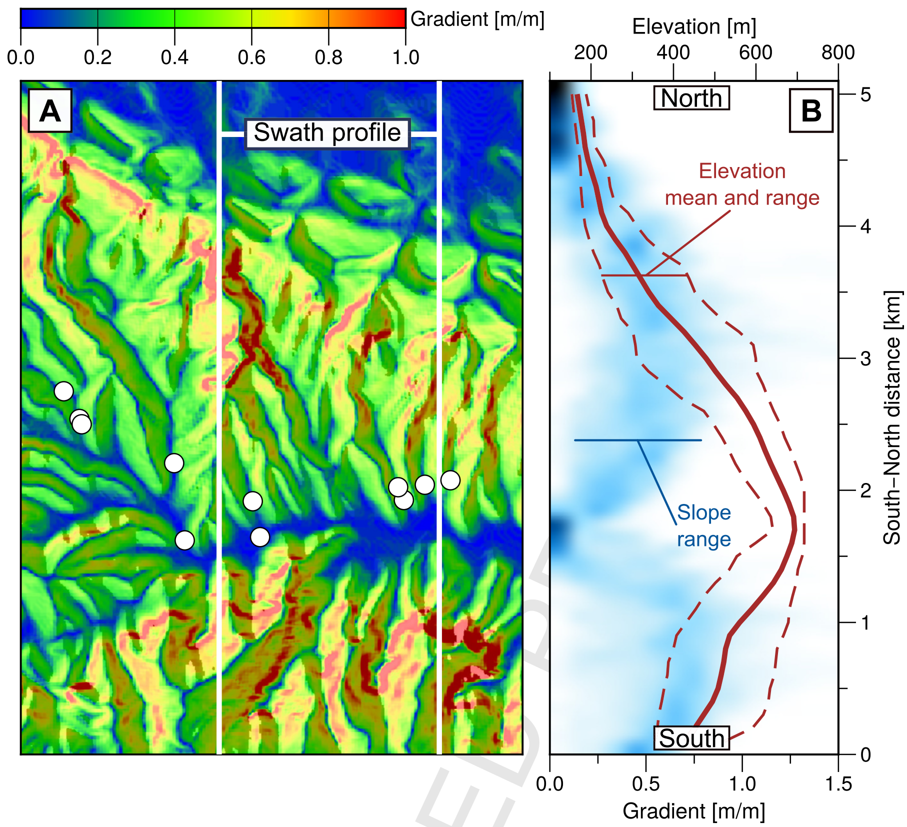

Fig. 8. A – Topographic gradient map over the main sampling area. Vertical bars indicate the width of the swath profile presented on inset B. White circles are sampling sites (Fig. 1C). B – North–south profile across the northern flank of the Petit Luberon. Red solid and dashed lines are the mean and extreme values of elevation. Intensity of blue background indicates the frequency distribution of hillslope gradients. (For interpretation of the references to color in this figure legend, the reader is referred to the web version of this article.)

bedrock (freeze-thaw cycles, biological agents) are only efficiently operating over a limited subsurface layer (<1 m) (Anderson et al., 2013).

Previous studies have shown that, in steady-state transport-limited landscapes dominated by linear slope-dependent regolith transport, the ratio between curvature and regolith production represents the efficiency of hillslope transport which is dimensionally equivalent to a diffusivity coefficient (e.g. Anderson, 2002). The apparent diffusion coefficient associated with the trend in our data is $\sim$0.002 m^2/yr. This value is in the lower range of the global compilation by Hurst et al. (2013b), but is consistent for the observed precipitation at our sites and significantly higher than values in arid environments. It is also one order of magnitude lower than values determined for the soil-mantled Mediterranean landscape of the Gabilan Mesa in Central California (Roering et al., 2007; Perron et al., 2012) and suggests that processes responsible for the mobilization of this coarse regolith are significantly less efficient than creep acting on a thick soil layer (McKean et al., 1993). The contrast between the incised flanks and the flat summit surface (Fig. 8) points to a transient evolution of the range and probably implies some degree of deviation from steady-state for the hillslopes. However, in the initial stages of their evolution (curvatures $<$0.02 m^{-1}), the near linear relationship between curvature and denudation strongly support the idea that hillslopes are closely following channel incision at their bottom and remain close to steady-state.

We note that the non-linear transport rule used in our modelling implies a much thinner regolith cover on the hillslope flank than on the hilltop when approaching the critical angle, which is not what we observed in the field. Such discrepancy suggests that this non-linear formulation is not adequately capturing some aspects of regolith transport in this kind of environments.

The limestone clasts produced by chemical and mechanical bedrock weathering are incorporated into the mobile regolith layer and then progressively transported downslope. Using the 0.01%/yr dissolution factor proposed above yields a characteristic time for the dissolution of 50% of clast mass of $\tau \simeq 7$ ka. Such survival over the 10 ka time-scale suggests that individual clasts produced at the hilltop are effectively moved away and transferred to the adjacent slopes over their life time.

5.3. Implications for relief evolution in carbonate landscapes

Our results have important implications for landscape evolution in carbonate-dominated settings, as they illustrate an abrupt limit of weathering processes to produce clasts and to lower the hillslope at a pace that matches the local base level fall. Such limitation of weathering below $\sim$70 mm/ka may prevent the hillslope/channel system from reaching an equilibrium shape and lead to an increase in hillslope relief. We observe such transient evolution in our study area where the lower parts of the range display near-threshold hillslope angles and high local relief, whereas the low-relief summit area is dominated by continuous slope-dependent hillslope evolution processes (Fig. 8). At a global scale we note that Mediterranean landscapes often display high local relief at 1–10 km wavelengths, with common occurrence of prominent limestone cliffs up to several hundred meters high. Our observations in the Luberon Mountains suggest that such relief could be a consequence of the inability of local weathering processes operating at the hillslope scale to keep pace with the dissection of topography by the fluvial network.

Ryb et al. (2013) report a significant change in landscape dynamics in the Judea Hills of Israel occurring around the mid-Pleistocene, from a situation where active landsliding was the dominant denudation process, toward hillslopes controlled by largely slope-independent dissolution. They interpret the present-day landscape as mostly inactive in terms of mechanical and gravity driven processes with long-wavelength features mostly inherited from the previous stage. The landscape of the northern flank of the Luberon mountain is in a transient state and dynamically adjusting during its evolution and we do not observe characteristics features of remnant topography such as large knickpoints or massive alluvial and colluvial deposits. The contrast between the near threshold hillslopes and cliffs of the lower part of the range and our studied area near the summit surface (Fig. 8) is a manifestation of the transition from a landscape dominated by diffusion dominated processes, toward a regime where hillslope failure and rapid mass movement assume a larger role in landscape evolution (Fig. 1C). We consider both parts to be active, and to represent two distinct stages in a progressive transient evolution of the range.

6. Conclusions

We have documented denudation across a carbonate range of South-Eastern France. Flat surfaces that are unaffected by gravity driven processes lower at 30–40 mm/ka, which is consistent with other observations on similar surfaces in peri-Mediterranean regions. While investigations of the relationship between hillslope convexity and denudation are almost as old as Geomorphology (Gilbert, 1909) and central to many hillslope evolution models, there is currently only a limited number of studies which document their co-evolution, and in particular the linear relationship we observe on Fig. 5. For our highest curvature sites we observe that denudation reaches a plateau at $\sim$60–70 mm/ka, which we interpret as a transition from transport-limited to weathering-limited evolution. Such change in behavior may promote the development of high local relief in Mediterranean landscapes as hillslopes become unable to match the imposed pace of base level lowering. Further investigations will attempt to address the dependence of the pattern we observe in Fig. 5 to different climatic settings in terms of precipitation and temperature.

Acknowledgements

This study was supported by the ECCOREV Research Federation and the Cashima Research Project (funded by the CEA Cadarache and ITER Organisation). We thank the Parc Naturel Régional du Luberon and the Office National des Forêts (ONF) for facilitating access to our field sites. The ^{36}Cl measurements were performed at the ASTER AMS national facility (CEREGE, Aix-en-Provence) which is supported by the INSU/CNRS, the ANR through the "Projets thématiques d'excellence" program for the "Equipements d'excellence" ASTER-CEREGE action, IRD and CEA. Simon Mudd, Bob Anderson, George Hilley and an anonymous reviewer are acknowledged for insightful comments on this manuscript.

References

Anderson, R.S., 2002. Modeling the tor-dotted crests, bedrock edges, and parabolic profiles of high alpine surfaces of the Wind River Range, Wyoming. Geomorphology 46 (1–2), 35–58. http://linkinghub.elsevier.com/retrieve/pii/S0169555X02000533.

Anderson, R.S., Anderson, S.P., Tucker, G.E., 2013. Rock damage and regolith transport by frost: an example of climate modulation of the geomorphology of the critical zone. Earth Surf. Process. Landf. 38 (3), 299–316. http://doi.wiley.com/10.1002/esp.3330.

Arnold, M., Aumaître, G., Bourlès, D.L., Keddadouche, K., Braucher, R., Finkel, R.C., Nottoli, E., Benedetti, L., Merchel, S., 2013. The French accelerator mass spectrometry facility ASTER after 4 years: status and recent developments on ^{36}Cl and ^{129}I. Nucl. Instrum. Methods Phys. Res., Sect. B, Beam Interact. Mater. Atoms 294, 24–28. http://linkinghub.elsevier.com/retrieve/pii/S0168583X12000924.

Carretier, S., Goddéris, Y., Delannoy, T., Rouby, D., 2014. Mean bedrock-to-saprolite conversion and erosion rates during mountain growth and decline. Geomorphology 209, 39–52. http://dx.doi.org/10.1016/j.geomorph.2013.11.025.

Clauzon, G., Fleury, T.J., Bellier, O., Molliex, S., Mocochain, L., Aguilar, J.P., 2011. Morphostructural evolution of the Luberon since the Miocene (SE France). Bull. Soc. Géol. Fr. 182 (2), 95–110.

Culling, W.E.H., 1960. Analytical theory of erosion. J. Geol. 68 (3), 336–344.

Dietrich, W.E., Bellugi, D.G., Sklar, L., Stock, J.D., Heimsath, A.M., Roering, J.J., 2003. Geomorphic transport laws for predicting landscape form and dynamics. In: Wilcock, P.R., Iverson, R.M. (Eds.), Prediction in Geomorphology. In: Geophys. Monogr., vol. 135. American Geophysical Union, Washington, DC, pp. 103–132. http://www.agu.org/books/gm/v135/.

Fifield, L., Ophel, T., Allan, G., Bird, J., Davie, R., 1990. Accelerator mass spectrometry at the Australian National University's 14UD accelerator: experience and developments. Nucl. Instrum. Methods Phys. Res., Sect. B, Beam Interact. Mater. Atoms 52 (3–4), 233–237. http://www.sciencedirect.com/science/article/pii/0168583X9090412N.

Foster, M.A., Anderson, R.S., Wyshnytzky, C.E., Ouimet, W.B., Dethier, D.P., 2015. Hillslope lowering rates and mobile-regolith residence times from in situ and meteoric ^{10}Be analysis, Boulder Creek Critical Zone Observatory, Colorado. Geol. Soc. Am. Bull. 127 (5), 862–878. http://gsabulletin.gsapubs.org/cgi/doi/10.1130/B31115.1.

Fuchs, M., 2007. An assessment of human versus climatic impacts on Holocene soil erosion in NE Peloponnese, Greece. Quat. Res. 67 (3), 349–356. http://linkinghub.elsevier.com/retrieve/pii/S0033589406001608.

Furlani, S., Cucchi, F., Forti, F., Rossi, A., 2009. Comparison between coastal and inland Karst limestone lowering rates in the northeastern Adriatic Region (Italy and Croatia). Geomorphology 104 (1), 73–81. http://www.sciencedirect.com/science/article/pii/S0169555X08002134.

Gilbert, G.K., 1909. The convexity of hilltops. J. Geol. 17 (4), 344–350. http://www.jstor.org/stable/30057970?_redirected.

Heimsath, A.M., Chappell, J., Dietrich, W.E., Nishiizumi, K., Finkel, R.C., 2000. Soil production on a retreating escarpment in southeastern Australia. Geology 28 (9), 787–790. http://geology.gsapubs.org/content/28/9/787.short.

Heimsath, A.M., Dietrich, W.E., Nishiizumi, K., Finkel, R.C., 1997. The soil production function and landscape equilibrium. Nature 388 (6640), 358–361.

Heisinger, B., Lal, D., Jull, A., Kubik, P., Ivy-Ochs, S., Knie, K., Nolte, E., 2002. Production of selected cosmogenic radionuclides by muons: 2. Capture of negative muons. Earth Planet. Sci. Lett. 200 (3–4), 357–369. http://www.sciencedirect.com/science/article/pii/S0012821X02006416.

Hoffman, B.S.S., Anderson, R.S., 2014. Tree root mounds and their role in transporting soil on forested landscapes. Earth Surf. Process. Landf. 39 (6), 711–722. http://doi.wiley.com/10.1002/esp.3470.

Hurst, M.D., Mudd, S.M., Attal, M., Hilley, G., 2013a. Hillslopes record the growth and decay of landscapes. Science 341 (6148), 868–871. http://www.sciencemag.org/content/341/6148/868.short.

Hurst, M.D., Mudd, S.M., Walcott, R., Attal, M., Yoo, K., 2012. Using hilltop curvature to derive the spatial distribution of erosion rates. J. Geophys. Res. 117 (F2), F02017. http://www.agu.org/pubs/crossref/2012/2011JF002057.shtml.

Hurst, M.D., Mudd, S.M., Yoo, K., Attal, M., Walcott, R., 2013b. Influence of lithology on hillslope morphology and response to tectonic forcing in the northern Sierra Nevada of California. J. Geophys. Res., Earth Surf. 118 (2), 832–851. http://doi.wiley.com/10.1002/jgrf.20049.

James, M.R., Robson, S., 2012. Straightforward reconstruction of 3D surfaces and topography with a camera: accuracy and geoscience application. J. Geophys. Res. 117 (F3), F03017. http://www.agu.org/pubs/crossref/2012/2011JF002289.shtml.

Johnstone, S.A., Hilley, G.E., 2015. Lithologic control on the form of soil-mantled hillslopes. Geology 43 (1), 83–86. http://geology.gsapubs.org/cgi/doi/10.1130/G36052.1.

McKean, J.A., Dietrich, W.E., Finkel, R.C., Southon, J.R., Caffee, M.W., 1993. Quantification of soil production and downslope creep rates from cosmogenic ^{10}Be accumulations on a hillslope profile. Geology 21 (4), 343–346. http://geology.gsapubs.org/content/21/4/343.short.

Merchel, S., Arnold, M., Aumaître, G., Benedetti, L., Bourlès, D., Braucher, R., Alfimov, V., Freeman, S., Steier, P., Wallner, A., 2008. Towards more precise ^{10}Be and ^{36}Cl data from measurements at the 10–14 level: influence of sample preparation. Nucl. Instrum. Methods Phys. Res., Sect. B, Beam Interact. Mater. Atoms 266 (22), 4921–4926. http://www.sciencedirect.com/science/article/pii/S0168583X08009476.

Molliex, S., Bellier, O., Terrier, M., Lamarche, J., Martelet, G., Espurt, N., 2011. Tectonic and sedimentary inheritance on the structural framework of Provence (SE France): importance of the Salon-Cavaillon fault. Tectonophysics 501 (1–4), 1–16. http://www.sciencedirect.com/science/article/pii/S0040195110003586.

Molliex, S., Siame, L.L., Bourlès, D.L., Bellier, O., Braucher, R., Clauzon, G., 2013. Quaternary evolution of a large alluvial fan in a periglacial setting (Crau Plain, SE France) constrained by terrestrial cosmogenic nuclide (^{10}Be). Geomorphology 195, 45–52. http://dx.doi.org/10.1016/j.geomorph.2013.04.025.

Mudd, S.M., Furbish, D.J., 2004. Influence of chemical denudation on hillslope morphology. J. Geophys. Res. 109 (F2), F02001. http://doi.wiley.com/10.1029/2003JF000087.

Pelletier, J.D., Barron-Gafford, G.A., Breshears, D.D., Brooks, P.D., Chorover, J., Durcik, M., Harman, C.J., Huxman, T.E., Lohse, K.A., Lybrand, R., Meixner, T., McIntosh, J.C., Papuga, S.A, Rasmussen, C., Schaap, M., Swetnam, T.L., Troch, P.A., 2013. Coevolution of nonlinear trends in vegetation, soils, and topography with elevation and slope aspect: a case study in the sky islands of southern Arizona. J. Geophys. Res., Earth Surf. 118 (2), 741–758. http://doi.wiley.com/10.1002/jgrf.20046.

Pelletier, J.D., Perron, J.T., 2012. Analytic solution for the morphology of a soil-mantled valley undergoing steady headward growth: validation using case studies in southeastern Arizona. J. Geophys. Res., Earth Surf. 117 (1), 1–11.

Perron, J.T., Kirchner, J.W., Dietrich, W.E., 2008. Spectral signatures of characteristic spatial scales and nonfractal structure in landscapes. J. Geophys. Res. 113 (F4), F04003. http://www.agu.org/pubs/crossref/2008/2007JF000866.shtml.

Perron, J.T., Richardson, P.W., Ferrier, K.L., Lapôtre, M., 2012. The root of branching river networks. Nature 492 (7427), 100–103. http://dx.doi.org/10.1038/nature11672.

Roering, J.J., 2008. How well can hillslope evolution models "explain" topography? Simulating soil transport and production with high-resolution topographic data. Geol. Soc. Am. Bull. 120 (9–10), 1248–1262. http://gsabulletin.gsapubs.org/cgi/doi/10.1130/B26283.1.

Roering, J.J., Almond, P., Tonkin, P., McKean, J., 2004. Constraining climatic controls on hillslope dynamics using a coupled model for the transport of soil and tracers: application to loess-mantled hillslopes, South Island, New Zealand. J. Geophys. Res. 109 (F1).

Roering, J.J., Kirchner, J.W., Dietrich, W.E., 1999. Evidence for nonlinear, diffusive sediment transport on hillslopes and implications for landscape morphology. Water Resour. Res. 35 (3), 853–870. http://www.agu.org/pubs/crossref/1999/1998WR900090.shtml.

Roering, J.J., Marshall, J., Booth, A.M., Mort, M., Jin, Q., 2010. Evidence for biotic controls on topography and soil production. Earth Planet. Sci. Lett. 298, 183–190.

Roering, J.J., Perron, J.T., Kirchner, J.W., 2007. Functional relationships between denudation and hillslope form and relief. Earth Planet. Sci. Lett. 264 (1–2), 245–258. http://dx.doi.org/10.1016/j.epsl.2007.09.035.

Ryb, U., Matmon, A., Erel, Y., Haviv, I., Benedetti, L., Hidy, A., 2014a. Styles and rates of long-term denudation in carbonate terrains under a Mediterranean to hyper-arid climatic gradient. Earth Planet. Sci. Lett. 406, 142–152. http://linkinghub.elsevier.com/retrieve/pii/S0012821X14005548.

Ryb, U., Matmon, A., Erel, Y., Haviv, I., Katz, A., Starinsky, A., Angert, A., Team, A., 2014b. Controls on denudation rates in tectonically stable Mediterranean carbonate terrain. Geol. Soc. Am. Bull. 126 (3–4), 553–568. http://gsabulletin.gsapubs.org/cgi/doi/10.1130/B30886.1.

Ryb, U., Matmon, A., Haviv, I., Benedetti, L., 2015. Exhumation and uplift coupled with precipitation along the western Dead Sea Rift margin. Geology 43 (6), 483–486. http://geology.gsapubs.org/cgi/doi/10.1130/G36331.1.

Ryb, U., Matmon, A., Porat, N., Katz, O., 2013. From mass-wasting to slope stabilization – putting constrains on a tectonically induced transition in slope erosion mode: a case study in the Judea Hills, Israel. Earth Surf. Process. Landf. 38 (6), 551–560.

Sadier, B., Delannoy, J.-J., Benedetti, L., Bourlès, D.L., Jaillet, S., Geneste, J.-M., Lebatard, A.-E., Arnold, M., 2012. Further constraints on the Chauvet cave artwork elaboration. Proc. Natl. Acad. Sci. USA 109 (21), 8002–8006. http://www.pnas.org/content/109/21/8002.

Schimmelpfennig, I., Benedetti, L., Finkel, R., Pik, R., Blard, P.-H., Bourlès, D., Burnard, P., Williams, A., 2009. Sources of in-situ ^{36}Cl in basaltic rocks. Implications for calibration of production rates. Quat. Geochronol. 4 (6), 441–461. http://www.sciencedirect.com/science/article/pii/S1871101409000910.

Schlagenhauf, A., Gaudemer, Y., Benedetti, L., Manighetti, I., Palumbo, L., Schimmelpfennig, I., Finkel, R., Pou, K., 2010. Using in situ Chlorine-36 cosmonuclide to recover past earthquake histories on limestone normal fault scarps: a reappraisal of methodology and interpretations. Geophys. J. Int. 182, 36–72.

Sharma, P., Kubik, P., Fehn, U., Gove, H., Nishiizumi, K., Elmore, D., 1990. Development of ^{36}Cl standards for AMS. Nucl. Instrum. Methods Phys. Res., Sect. B, Beam Interact. Mater. Atoms 52 (3–4), 410–415. http://www.sciencedirect.com/science/article/pii/0168583X90904473.

Siame, L., Bellier, O., Braucher, R., Sébrier, M., Cushing, M., Bourlès, D., Hamelin, B., Baroux, E., de Voogd, B., Raisbeck, G., Yiou, F., 2004. Local erosion rates versus active tectonics: cosmic ray exposure modelling in Provence (south-east France). Earth Planet. Sci. Lett. 220 (3–4), 345–364. http://dx.doi.org/10.1016/S0012-821X(04)00061-5.

Small, E.E., Anderson, R.S., Hancock, G.S., 1999. Estimates of the rate of regolith production using ^{10}Be and ^{26}Al from an alpine hillslope. Geomorphology 27 (1–2), 131–150. http://dx.doi.org/10.1016/S0169-555X(98)00094-4.

Stone, J., Allan, G., Fifield, L., Evans, J., Chivas, A., 1994. Limestone erosion measurements with cosmogenic chlorine-36 in calcite — preliminary results from Australia. Nucl. Instrum. Methods Phys. Res., Sect. B, Beam Interact. Mater. Atoms 92 (1–4), 311–316. http://www.sciencedirect.com/science/article/pii/0168583X94960259.

Stone, J.O., 2000. Air pressure and cosmogenic isotope production. J. Geophys. Res. 105 (B10), 23753–23759. http://www.agu.org/pubs/crossref/2000/2000JB900181.shtml.

Westoby, M., Brasington, J., Glasser, N., Hambrey, M., Reynolds, J., 2012. 'Structure-from-Motion' photogrammetry: a low-cost, effective tool for geoscience applications. Geomorphology 179, 300–314. http://dx.doi.org/10.1016/j.geomorph.2012.08.021.

Yoo, K., Mudd, S.M., Sanderman, J., Amundson, R., Blum, A., 2009. Spatial patterns and controls of soil chemical weathering rates along a transient hillslope. Earth Planet. Sci. Lett. 288 (1–2), 184–193.

Sponsor names

Do not correct this page. Please mark corrections to sponsor names and grant numbers in the main text.

Q12

CEA, *country*=France, *grants*=

ANR, *country*=France, *grants*=

CEA, *country*=France, *grants*=

Contents lists available at ScienceDirect
Earth and Planetary Science Letters
www.elsevier.com/locate/epsl

Graphical abstract

Earth and Planetary Science Letters ●●●●, ●●●, ●●●

Weathering-limited hillslope evolution in carbonate landscapes

Vincent Godard[a,*], Vincent Ollivier[b], Olivier Bellier[a], Cécile Miramont[c], Esmaeil Shabanian[a], Jules Fleury[a], Lucilla Benedetti[a], Valéry Guillou[a], ASTER Team[a]

[a] Aix-Marseille Université, CNRS, IRD, CDF, CEREGE UM34, 13545 Aix-en-Provence, France
[b] Aix Marseille Université, CNRS, MCC, LAMPEA UMR 7269, 13094 Aix-en-Provence, France
[c] Aix-Marseille Université, CNRS, IRD, Avignon Université, IMBE UMR 7263, 13545 Aix-en-Provence, France

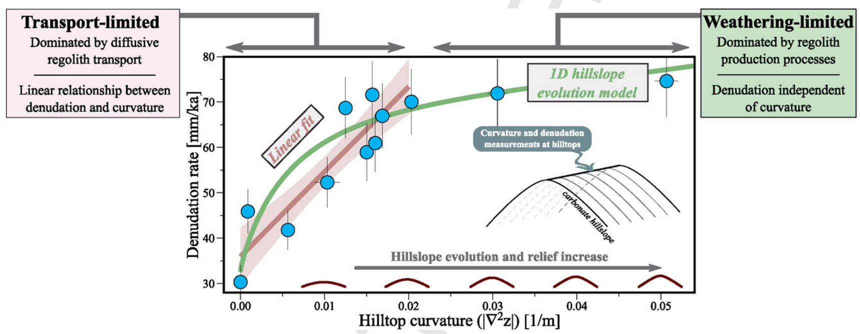

Please cite this article in press as: Godard, V., et al. Weathering-limited hillslope evolution in carbonate landscapes. Earth Planet. Sci. Lett. (2016), http://dx.doi.org/10.1016/j.epsl.2016.04.017

Highlights

- We measure the evolution of curvature with denudation on hilltops of a carbonate range.
- For low curvature ridges we observe a linear increase of denudation with curvature.
- For high curvature ridges denudation becomes nearly constant and independent of curvature.
- This suggests a transition from transport to supply limited dynamics.

Please cite this article in press as: Godard, V., et al. Weathering-limited hillslope evolution in carbonate landscapes. Earth Planet. Sci. Lett. (2016), http://dx.doi.org/10.1016/j.epsl.2016.04.017